The Journal of Experimental Biology 214, 3082-3095

doi:10.1242/jeb.051110

RESEARCH ARTICLE

Subglottal pressure and fundamental frequency control in contact calls of juvenile *Alligator mississippiensis*

Tobias Riede[1,2,*], Isao T. Tokuda[3] and C. G. Farmer[1]

[1]Department of Biology, University of Utah, Salt Lake City, UT 84112, USA, [2]National Center for Voice and Speech, University of Utah, Salt Lake City, UT 84112, USA and [3]Department of Micro System Technology, Ritsumeikan University, 1-1-1 Nojihigashi, Kusatsu, Shiga 525-8577, Japan

*Author for correspondence (t.riede@utah.edu)

Accepted 21 April 2011

SUMMARY

Vocalization is rare among non-avian reptiles, with the exception of the crocodilians, the sister taxon of birds. Crocodilians have a complex vocal repertoire. Their vocal and respiratory system is not well understood but appears to consist of a combination of features that are also found in the extremely vocal avian and mammalian taxa. Anatomical studies suggest that the alligator larynx is able to abduct and adduct the vocal folds, but not to elongate or shorten them, and is therefore lacking a key regulator of frequency, yet alligators can modulate fundamental frequency remarkably well. We investigated the morphological and physiological features of sound production in alligators. Vocal fold length scales isometrically across a wide range of alligator body sizes. The relationship between fundamental frequency and subglottal pressure is significant in some individuals at some isolated points, such as call onset and position of maximum fundamental frequency. The relationship is not consistent over large segments of the call. Fundamental frequency can change faster than expected by pressure changes alone, suggesting an active motor pattern controls frequency and is intrinsic to the larynx. We utilized a two-mass vocal fold model to test whether abduction and adduction could generate this motor pattern. The fine-tuned interplay between subglottal pressure and glottal adduction can achieve frequency modulations much larger than those resulting from subglottal pressure variations alone and of similar magnitude, as observed in alligator calls. We conclude that the alligator larynx represents a sound source with only two control parameters (subglottal pressure and vocal fold adduction) in contrast to the mammalian larynx in which three parameters can be altered to modulate frequency (subglottal pressure, vocal fold adduction and length/tension).

Key words: vocal folds, Sauropsida, two-mass model, phonation threshold pressure, syrinx, pulse register.

INTRODUCTION

Crocodilia have evolved more complex vocal behaviors than Lepidosauria or Chelonia within the diverse group of Reptilia. The complexity is manifested by more frequent vocalization, larger vocal repertoires, and the ability to modulate fundamental frequency (F_0) and sound amplitude (e.g. Young, 2003; Wang et al., 2007; Vergne et al., 2009). The alligator vocal organ and respiratory system contains features that are also found in much more vocal taxa, such as birds, frogs and mammals. The respiratory system is very bird like in that airflow through the gas-exchanging parenchyma is unidirectional (Farmer and Sanders, 2010) and the respiratory system is very compliant (Perry and Duncker, 1980). Unlike birds, the alligator's primary sound source, however, is the larynx, and there are no features that are remininscent of a syrinx. Two laterally positioned vocal folds inside the larynx of the alligator can be set into vibration if air is blown through the organ (Müller, 1839) and intrinsic laryngeal muscles can abduct and adduct them, but a tension mechanism is presumably missing (Henle, 1839; Göppert, 1899; Göppert, 1937; Söller, 1931; Reese, 1945; Vogel, 1976). It is unclear how alligators produce a F_0 modulation with such a larynx. Are abduction and adduction sufficient to achieve the observed frequency modulation? A better understanding of the production mechanism will provide further details about the alligator's complex vocal behavior and could shed light on the evolution of the larynx as a vocal organ. From lungfish to mammals, abduction and adduction are the most critical function of any larynx, fulfilling its respiratory valve function. Yet a large step for the evolution of the larynx as a vocal organ towards increased complexity is the evolution of a tensor mechanism that extends the frequency range that can be produced.

Alligators produce a variety of call types (e.g. Herzog and Burghardt, 1977; Vliet, 1989; Wang et al., 2007; Vergne et al., 2009). Contact calls (Vergne et al., 2009) [also termed the 'distress call' (Herzog and Burghardt, 1977)] are frequently uttered by juvenile alligators in various contexts. They show a harmonic structure. The maximum F_0 can be as high as 1 kHz; the lowest frequency is around 50 Hz, usually at the end of the call.

In the current study we conducted three different experiments. First, we investigated how vocal fold length in the alligator larynx scales with body size. Morphological specializations (for example larger or smaller size than expected by isometric scaling) in vertebrate sound sources are usually a manifestation of a functional adaptation.

Second, we recorded subglottal pressure (P_s) and sound during contact call production to study the relationship between P_s, F_0 and sound amplitude. Sound produced by flow-induced vocal fold vibrations is critically dependent on P_s. P_s variations can contribute to modulate the vocal fold's oscillation rate; however, the extent of this effect is limited (Titze, 1989a).

Our measurements indicated that F_0 is not solely regulated by P_s. We therefore, in a third approach, used a computer model to test whether the adductive mechanism, present in the alligator larynx, can achieve frequency modulations as in a contact call. A two-mass vocal fold model capturing the essential elements of flow-induced vocal fold oscillation and considering P_s data from the juvenile alligators was capable of maintaining phonation and simulating frequency modulations with P_s and adduction as the only variables.

Terminology and alligator larynx morphology

We use the term 'vocal fold' to refer to the laterally positioned masses of connective tissue which are involved in sound production. In the alligator literature, various terms for this structure can be found, such as Stimmband (Henle, 1839) or Labien (Müller, 1839) in the German literature, or vocal cord and/or fold (Reese, 1915) in the English literature. Throughout this text we use the term vocal fold for the entirety of the structure involved in oscillation. It is a more generic and all-encompassing term than the term vocal cord, which should remain reserved to a band of organized connective tissue inside the vocal fold, also known as the ligamentum vocale. The presence of a ligamentum vocale is species specific. It is unknown whether it exists in alligators. Using an excised larynx setup, Müller observed that vocal folds of American alligators start to oscillate if air is blown through the trachea and larynx (Müller, 1839). He noted: 'Diese dicken Labien gerathen beim Blasen durch die Luftröhre ganz so, wie die Stimmbänder des Menschen in Schwingung.' (English translation: 'These thick labia start to vibrate just like the vocal folds of humans if air is blown through the trachea.') [see p. 44 of Müller (Müller, 1839)].

The alligator's larynx consists of three types of cartilage (Fig. 1A), two groups of muscles, connective tissue, epithelium and a branch from the vagus nerve. The cricoid cartilage is a ring structure at the cranial end of the trachea. The two arytenoid cartilages are long structures each shaped like a semi-circle (Fig. 1). The two ends of the semi-circle connect dorsally (*via* a ligamentous connection) and ventrally (*via* a crico-arytenoid articulation) to the cricoid cartilage allowing latero-lateral movement of the arytenoid cartilages. Two intrinsic laryngeal muscles are responsible for opening and closing the glottis (Table 1). The constrictor consists of two portions: a sphincter glottidis and a sphincter aditus laryngis (Fig. 1). The cricoarytenoid muscle pulls the arytenoid cartilages laterally, thereby opening the glottis. The arytenoid cartilages lie embedded in the vocal folds, allowing latero-lateral movements effected by the two portions of the constrictor muscle and the cricoarytenoid muscle (Fig. 1D).

Henle (Henle, 1839) and later Söller (Söller, 1931) suggested the upper (dorsal) and a lower (ventral) portions of the space between vocal folds differ. This differentiation is based on a suspected functional separation of two portions of the constrictor muscle, which might independently adduct the lower and upper part of the vocal folds. There is no true aditus laryngis as in mammals and therefore we refer to the space between the left and right vocal fold uniformly as glottis, but acknowledge the possibility of a differentiated abduction/adduction mechanism. The vocal folds open cranially into a large space consisting of the pharyngeal area and upper part of the esophagus. This space can be enormously expanded during a maneuver known as gular pump. The hyoid cartilage can be moved up and down, affecting the size of the supraglottal esophago-pharyngeal space, a movement with relevance for respiration (Owerkowicz et al., 1999) and maybe also in sound production, as in birds (Riede et al., 2006).

The subglottal area shows first two lateral cavities (hereafter 'subglottal lateral ventricle') that are formed by the dorsal branch of the arytenoid cartilage and the lateral wall of the larynx. The cricoid cartilage sits caudal from the arytenoid cartilages. It possesses two laterally extended large chambers. They do not resemble the bulla-like extensions in primates or bats (Riede et al., 2008), but represent an overall extended space confined by the cricoid cartilage.

The larynx is placed inside the cup-like hyoid cartilage. A flap [termed 'mouth flap' by Negus (Negus, 1949) and 'lower flap' by Ferguson (Ferguson, 1981)] posterior to the tongue (consisting of the cranial edge of the hyoid cartilage and overlaid with a thin layer of connective tissue and epithelium) can be brought in firm contact with the palate. There is an opposing upper flap descending from the palate (Ferguson, 1981) that can form a watertight seal separating the oral cavity from the pharynx, thereby preventing water from reaching the larynx (Ferguson, 1981; Reese, 1945). Air flows from the nostrils along the nasal passage, formed dorsally from the primary palate and ventrally by the secondary palate, to the glottis so that the animal can breathe (or vocalize) with its mouth under water and the nares above the surface of the water. The glottis can probably be placed near the naso-pharyngeal duct, maybe even pressed firmly against it, as in some birds (Zweers et al., 1981), but not inserted into the nasal cavity, like the nasopharyngeal junction in some mammals, e.g. rhinolophid bats.

During vocalization, air flows through the nares. No anatomical structure exists that could actively constrict and affect the airflow between the glottis and nares. The nares are wide open during vocalization, which leaves the glottis as the main regulator of airflow in the respiratory system. The nares are rather small and we therefore assume that some of the sound is radiated through the skin. During the vocalizations investigated in this study, the oral flap was always closed. However, we observed that sometimes, when not submerged, animals vocalize with this seal open. The acoustic properties of such a call are very different.

Table 1. Intrinsic laryngeal muscles of the alligator

Muscle	Origin	Insertion	Function	Innervation
Musculus cricoarytenoideus (Söller, 1931) [synonymous with dilator laryngis (Göppert, 1937)]	Caudo-lateral on cricoid and first tracheal ring	Processus medialis, i.e. dorso-lateral portion of cricoid	Opening the glottis	Ventral branch of the larynx branch of the vagus nerve
Constrictor laryngis				
Sphincter aditus laryngis	Ventral raphe and frontal edge of cricoid and lateral surface of cricoid	Dorsal raphe accepts fibers from front, back and lateral	Closing the upper part of the glottis	Dorsal branch of the larynx branch of the vagus nerve
Sphincter glottidis			Closing the lower part of the glottis	Ventral branch of the larynx branch of the vagus nerve

After Söller (1931) and Göppert (1937); confirmed by our own preparations.

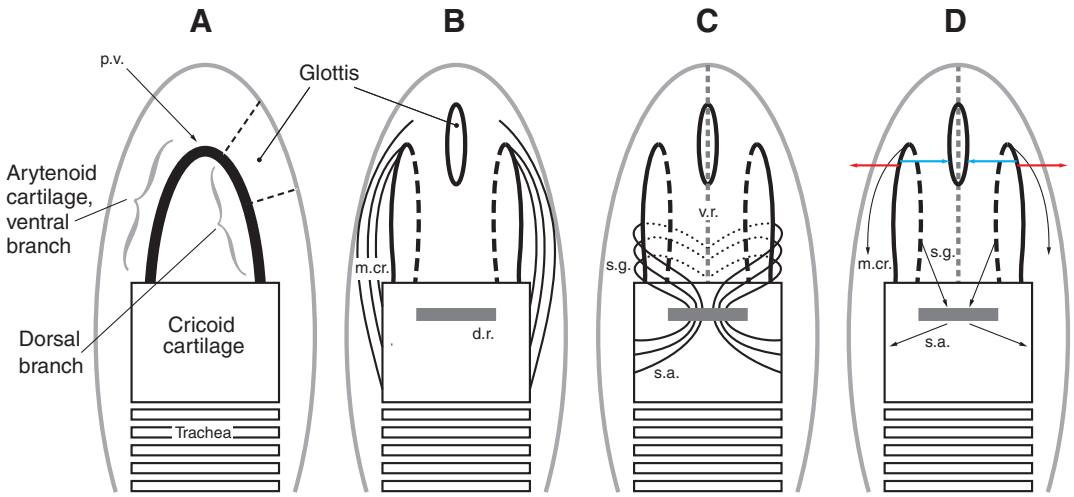

Fig. 1. Schematic illustration of the alligator's larynx morphology in lateral view (A) and in top view (B–D). The cricoid cartilage is a closed ring at the cranial end of the tracheal tube. The arytenoid cartilages are two half-rings positioned laterally. They connect with the cricoid cartilage at a ventral and dorsal point, and their arch points rostrally. In B–D, the dorsal branches of the arytenoid cartilages are indicated by a solid line which continues as a dashed line, indicating the ventral branch. The abductor muscle (m.cr., musculus cricoarytenoideus) reaches from lateral of the cricoid cartilage to the most cranial point of the arytenoid cartilages (p.v., processus vocalis). A contraction will cause a lateral movement (indicated by red arrows in D) of the arytenoid cartilages. The constrictor muscle consists of two portions (s.g., sphincter glottidis; s.a., sphincter aditius) inserting into a dorsal raphe (d.r.). The sphincter glottidis reaches around the arytenoid cartilages and meets medially in a ventral raphe (v.r.). A contraction causes a medial movement of the arytenoid cartilages (indicated by blue arrows in D).

MATERIALS AND METHODS

Morphology

Thirty-three *Alligator mississippiensis* (Daudin 1802) larynges were retrieved to investigate how vocal fold length scales with body size. Twenty female larynges were provided by the Alligator Tissue Bank at UC Irvine (courtesy of Tomasz Owerkowicz and Jim Hicks). One male larynx was provided by Ruth Elsey (Rockefeller Wildlife Refuge, LA, USA). Four male larynges were provided by the University of Utah Vertebrate Evolution lab. In these animals, body mass and snout–vent length were available. Eight larynges (from four males and four females) were provided by John V. Price (Insta-Gator, Ranch & Hatchery, LA, USA), from which only body masses were available.

Two female and two male larynges (1–2 kg alligators) were used for histology. The isolated tissue was stored in 10% buffered formalin phosphate (Fisher Scientific, Fair Lawn, NJ, USA; cat. no. SF100-4) and then placed for 8 h in Decalcifier 1® (Surgipath Medical Industries Inc., Richmond, IL, USA; cat. no. 00400) before further processing. The tissue was then embedded in paraffin and 5 µm cross-sections were made at six subsequent levels from the cranial to the caudal end of the larynx. Sections were stained with hemotoxylin and eosin for a general histological evaluation.

Computer tomographic images of an inspiratory phase of a normal respiratory cycle became available through a different study (Farmer and Sanders, 2010), allowing the investigation of vocal fold shape. A 128 slice dual energy Siemens (New York, NY, USA) SOMATOM definition computed tomography unit was used to collect data from an 11 kg alligator during a natural respiration.

P_s measurements

All procedures were reviewed and approved by the Institutional Animal Care and Use (IACUC) committee of the University of Utah.

Seven alligators ranging in size between 31 and 37 cm (snout–vent length) and 0.9 and 1.4 kg body mass, 3 years of age, were used for the study. One animal vocalized little before and only twice during the experiment and was therefore removed from further analysis. Animals were housed in a 200 l plastic container under a natural light regimen. Animals were fed *ad libitum* twice a week. Water temperature averaged 18°C.

For the experiment an animal was placed in a 2×2 m arena equipped with a 50 l water basin. A heat lamp was placed over the arena opposite to the water basin providing a 14 h/10 h light cycle. The animals were fed daily (Mazuri® Crocodilian Diet). The study period for each animal lasted 14 days.

P_s was measured with a Millar pressure sensor (PCU-2000 control unit and SPR-524 sensor; Houston, TX, USA), which was calibrated before each experiment with a U-tube manometer and the calibration checked after the experiment. The sensor was placed intratracheally about 2 cm caudally from the glottis. Under visual control, it was guided transorally through the glottis into the trachea. This procedure followed a setup used in humans (van den Berg, 1956; Cranen and Boves, 1985). The catheter tip position relative to the airflow direction can have a small effect on pressure values. For a test, air was blown through a 50 cm long Silastic tube (1 cm inner diameter) at 20 and 60 l min^{-1}. The sensor was placed at 0 deg (parallel), at 45 deg and at 90 deg (perpendicular) to the airflow. The standard deviation of pressure measurements between the three positions was 0.012 kPa (0.6%) at the lower flow rate and 0.019 kPa (0.29%) at the higher flow rate.

The sensor cable (o.d. 0.7 mm) was protected from the animal's teeth by feeding it through a curved plastic tube (o.d. 2.8 mm). The tube was fixed to the animal's upper jaw/snout with several layers of duct tape. The plastic tube was fixed to the animal 2 days before the pressure sensor was implanted for the animal to adapt to the presence of the tube. All animals resumed spontaneous vocalization within those 2 days. The lower jaw was freely moveable and feeding was not prevented by the plastic tube or the pressure sensor. The animals wore a jacket around the thorax, which enabled the attachment of the sensor and a flexible leash, which was fixed 1 m above the cage and allowed the animal free movement in the cage.

Table 2. Raw data of three fundamental frequency parameters (F_0 call onset; F_0 call end; maximum F_0), three subglottal pressure parameters (P_s call onset; P_s call end; P_s at maximum F_0) and call duration in 'begging calls'

ID no.	BM (kg)	SVL (cm)	F_0 call onset (Hz)	F_0 call end (Hz)	Maximum F_0 (Hz)	P_s call onset (kPa)	P_s call end (kPa)	P_s at maximum F_0 (kPa)	Call duration (ms)	P_s increase (kPa)
736	0.9	32	569±166	52±25	572±164	2.7±0.9	1.7±0.2	2.8±0.9	117±31	1.7±0.8
(*N*=22)			243–839	24–125	243–839	1.1–4.1	1.0–2.0	1.1–4.3	80–199	
741	1.3	36	587±250	63±28	589±251	3.4±1.1	2.0±0.5	3.9±1.4	123±40	2.4±1.4
(*N*=22)			215–1012	18–142	215–1012	1.9–5.8	1.0–2.9	2.1–6.5	66–277	
738	1.3	38.5	621±476	52±35	772±410	2.6±1.6	1.9±1.0	3.5±1.6	202±75	2.1±1.4
(*N*=22)			110–1622	18–166	186–1622	1.1–7.8	1.0–5.3	1.6–8.1	86–366	
737	1.5	37	209±128	69±68	223±126	2.3±1.3	1.9±0.7	2.5±1.0	271±226	0.7±0.5
(*N*=22)			66–580	5–268	90–580	1.0–5.6	0.7–3.4	1.4–5.6	49–974	
749	1.5	38.5	350±189	116±69	403±231	1.0±0.4	1.1±0.4	1.7±0.9	202±151	1.5±0.9
(*N*=12)			100–681	22–220	27–757	0.5–1.8	0.4–2.0	0.8–4.1	57–589	
742	1.3	38	235±141	48±17	257±103	2.1±0.4	1.7±0.5	2.5±0.6	287±200	1.7±0.9
(*N*=4)			40–344	34–71	125–344	1.9–2.7	1.1–2.4	1.7–3.1	72–475	

Means ± s.d.; range: minimum–maximum. First column indicates alligator identification and number of calls (*N*) from each individual. BM, body mass; SVL, snout–vent length; P_s increase, subglottal pressure increase during a 100 ms period before phonation onset.

The transglottal positioning of tube-like devices is irritating during the moment of entering and passing the glottis; however, once the device was positioned, normal breathing, swallowing and feeding resumed. The transglottally positioned sensor could have affected the normal process of phonation by disturbing vocal fold oscillation and/or the tight closure of the glottis. However, four observations suggest that the procedure applied here did not affect phonation or breathing. (1) Visual inspection confirmed that the wire was positioned in the ventral commissure of the glottis. In mammals, vocal folds show their largest oscillation amplitudes in the middle. Smaller or no oscillation can be seen toward the ventral and dorsal end. A ventral positioning of the wire should therefore affect the oscillation amplitude the least. (2) We observed no glottal leak during respiration. The alligator's respiratory cycle is characterized by a long holding phase after the inspiration at elevated P_s (Farmer and Carrier, 2000a; Farmer and Carrier, 2000b; Claessens, 2009). This typical cycle could be observed in all study subjects, and no unnatural pressure drop was observed. (3) The sounds produced with the pressure sensor inserted were similar to spontaneous vocalization during unrestricted behavior in all acoustic variables. (4) The sensor, which was in place for between 3 and 6 days, did not cause respiratory problems. In particular, during feeding no signs such as coughing, food refusal or elevated respiratory rate above normal were observed.

In one animal we implanted a microbead thermistor (0.13 mm, BB05JA202; Thermometrics, Northridge, CA, USA) to measure flow and a Millar pressure transducer to measure P_s, both percutaneously. Prior to surgery, the alligator was anesthetized with isoflurane (VetOne, Meridiane, ID, USA). The trachea was exposed through a skin incision (in the midline, ~10 cm caudal from snout), and the trachea was exposed. The pressure transducer was inserted between two tracheal rings (about 2 cm below the larynx) and anchored by a suture to one of the rings. Tissue adhesive was used to prevent air leaks. Caudal to the transducer, a flow thermistor was implanted. The flow probe was inserted into the trachea about 2 mm caudal from the pressure transducer, also between two tracheal rings. Wires were led through the skin and routed to microconnectors on the backpack. The rate of airflow through the trachea was determined by a feedback circuit in which the current needed to maintain a heated thermistor at a constant temperature was proportional to the rate of airflow (Hector Engineering, Ellettsville, IN, USA). The procedure was performed only in one animal because the recovery period was longer than in the transglottal procedure (normal behavior including vocalization returned after about 48 h). However, we deem the insights gained from this single attempt worthwhile to report.

The animals uttered spontaneous vocalizations most reliably during feeding time. We recorded and analysed 'contact calls' (Vergne et al., 2009). Two weeks before implantation of the sensor, the experimenter conditioned the animal by sitting next to the cage and providing food every time the animal called. Within 2–4 days, animals responded when the experimenter entered the room by approaching and vocalizing. Once the animal's response was stable, the implantation was performed.

Vocalizations were recorded with a Sennheiser microphone (ME80 head with K3U power module; Old Lyme, CT, USA). The pressure signal and the sound signal were simultaneously recorded with a BioPac System (Goleta, CA, USA; AcqKnowledge acquisition software, BioPac) at 40 kHz sampling frequency.

Data were analyzed based on narrowband spectrograms and measurements therein using Praat (Boersma and Weenick, 2008). Sounds recorded before sensor implantation were analyzed for call duration and F_0 at the beginning, at its maximum and at the end of a call. Measurements were made from 20 calls per individual in four individuals and from fewer than 20 calls in two individuals (Table 2).

Post-surgery recordings were analyzed for F_0, P_s, sound intensity level (SIL) and call duration. The sound signal was band-pass filtered between 70 and 5000 Hz, and F_0 and SIL contours were calculated with Praat functions ('show formants' and 'show intensity') and confirmed by visual inspection. The P_s signal was down-sampled to 100 Hz. All three variables were calculated at 7.5 ms intervals, and were aligned with call duration.

Three tests were performed to investigate the relationship between F_0 and P_s more closely. First, we tested whether P_s is correlated with F_0 at call onset, at maximum F_0 and at call offset. The Pearson correlations were calculated for each individual separately.

Second, we compared the contours of F_0, P_s and SIL. Parameters were normalized to maximum in the respective call, allowing comparisons between individuals. The contours were then estimated with 2nd degree polynominal models. The time points at which the maxima of F_0, P_s and SIL occur were estimated by calculating the zero for the polynominal models. An average polynominal model across six individuals was also calculated by taking the mean of the constants a, b and c.

Third, the frequency change achieved per 1 kPa was estimated. F_0 change due to P_s variation is limited. In mammalian larynges, P_s alone (keeping vocal fold stiffness constant) can account for F_0 changes of ~10–50 Hz per 1 kPa pressure change (Titze, 1989a). In zebra finches, P_s alone can account for F_0 changes between 5 and 40 Hz per 1 kPa (Riede et al., 2010a). We calculated the F_0 change per kPa pressure change for call segments between the time of maximum pressure (usually early in a call) and the end of a call. Calls in which a frequency change of less than 20 Hz or a non-uniform pressure change was observed were excluded.

Computer simulation

Müller was able to trigger vocal fold oscillations in an excised alligator larynx (Müller, 1839), indicating that voice production in alligators is also a consequence of the flow-induced vibrations of the vocal folds. We assume that the basic mechanism of flow-induced vibrations is similar to that in vocal fold oscillation in humans/mammals (e.g. Flanagan, 1972): with the vocal folds at rest, lung pressure increases, forcing the vocal folds apart. As the glottis opens, Bernoulli's law can be used to relate pressure and velocity. A convergent cross-sectional area of the vocal folds is essential for the oscillation to occur. Velocity increases in the convergent part of the glottis while pressure decreases. Pressure decreases up to the point of flow separation in the divergent part of the glottis approaching supraglottal pressure levels (Jiang and Titze, 1994). Now viscous effects become dominant as the folds move towards the midline, resulting in a decrease in flow velocity. The pressure in the upstream region of the glottis increases if the flow stops, which counters the closure. This pressure again forces the folds apart, and the cycle repeats itself. Titze indicated that as long as intraglottal pressure is greater during the opening phase than during the closing phase there will be a positive transfer of energy from the airflow to the vocal folds (Titze, 1988b). A positive value is required to overcome damping within the vocal fold tissue. The energy flow from the air stream to the vocal folds is roughly equivalent to the force exerted on the vocal folds by the normal pressure, multiplied by the normal component of velocity.

We applied this basic mechanism to further investigate possible laryngeal maneuvers that could modulate F_0 as observed in the alligators. Traditionally, three parameters are usually implemented in vocal fold models in order to change F_0: (1) adduction, (2) vocal fold tension and (3) P_s. Anatomical studies have not yet identified a tensor mechanism in alligators. Our pressure measurements (see Results) indicate that an active laryngeal mechanism must accompany alligator phonation. We therefore utilized a computational model to investigate the possibility that with two parameters (adduction and P_s) a frequency modulation of similar magnitude to that in alligator calls can be achieved.

The two-mass model (Ishizaka and Flanagan, 1972; Steinecke and Herzel, 1995) was implemented as the computational model of the vocal folds. The idea of the two-mass model is to divide the vocal fold tissue into upper and lower portions of masses, which are coupled by springs (Fig. 2). This enables simulation of the core mechanism of the vocal fold vibration, which is the phase shift of the lower and upper edges of the vocal folds. This movement is essential for realizing an efficient energy transfer from glottal airflow to vocal fold tissue (Titze, 1988b). The simplified model with few masses, which has been successfully applied to study various aspects of the human voice (e.g. Tokuda et al., 2007; Tokuda et al., 2010), represents a compromise between the representation of the most basic mechanism of flow-induced tissue oscillation and the limited knowledge about muscle activity, exact flow rates and vocal fold oscillation characteristics.

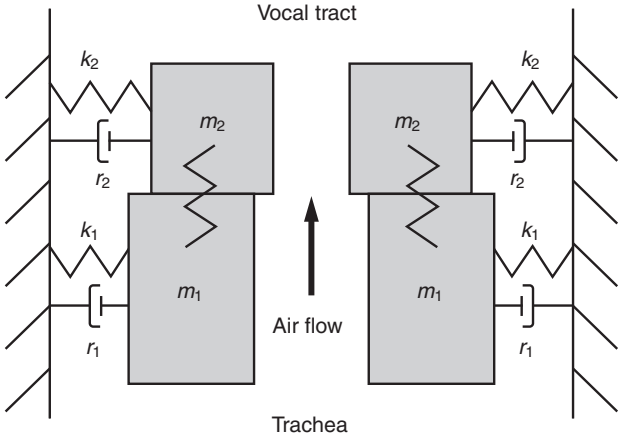

Fig. 2. Schematic illustration of the two mass model. The left and right vocal folds have a symmetric configuration. Each vocal fold is composed of a lower mass (m_1) and an upper mass (m_2), which are coupled by linear springs. The airflow coming from the lung is described by Bernoulli's principle below the narrowest part of the glottis. k_i, stiffening of the lower and upper masses; r_i, damping of the lower and upper masses; i=1,2.

Fig. 2 shows a schematic representation of the vocal fold model. m_1 and m_2 represent lower and upper masses, respectively. Letting $x_{1\alpha}$ and $x_{2\alpha}$ be displacements of the lower and upper masses with the index denoting either left or right side (α=l,r), the equation of motion is derived as:

$$m_1\ddot{x}_{1\alpha} + r_1\dot{x}_{1\alpha} + k_1x_{1\alpha} + \Theta(-a_1)c_1(a_1/2l) + k_c(x_{1\alpha} - x_{2\alpha}) = ld_1P_1 ,$$

$$m_2\ddot{x}_{2\alpha} + r_2\dot{x}_{2\alpha} + k_2x_{2\alpha} + \Theta(-a_2)c_2(a_2/2l) + k_c(x_{2\alpha} - x_{1\alpha}) = ld_2P_2 , \quad (1)$$

where k_i and r_i stand for stiffness and damping of the lower and upper masses (i=1,2), whereas k_c stands for mutual coupling between the two masses. Lower and upper glottal areas are given by a_i=l(x_0+x_{ir}+x_{il}), where x_0 represents arytenoid distance and l

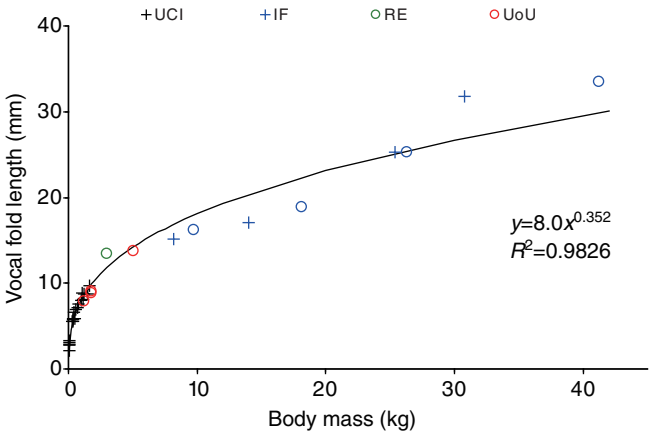

Fig. 3. The vocal fold length of alligators, when plotted against body mass, falls close to a line with a slope of 0.35. Data were collected from four different populations: Alligator Tissue Bank at UC Irvine (UCI); Insta-Gator Ranch and Farm (IF); Rockefeller Wildlife Refuge (RE); and University of Utah Vertebrate Evolution lab (UoU). Females (crosses) and males (circles) are indicated separately. Regression function and coefficient (r^2) are shown and were calculated by pooling data from males and females from all four populations.

corresponds to the vocal fold length. c_i describes collision force, which is activated during glottal closure, where the activation function is defined as $\Theta(x)=1$ ($x>0$), 0 ($x<0$). For simplicity, symmetric motion between the left and right vocal folds is assumed ($x_{1l}=x_{1r}$, $x_{2l}=x_{2r}$). The effect of vocal tract acoustic loading is not considered.

Under the assumption that the flow inside the glottis obeys the Bernouli principle below the narrowest part of the glottis, pressure that acts on each mass is given by $P_1=P_s\{1-\Theta(a_{min})(a_{min}/a_1)^2\}\Theta(a_1)$, $P_2=0$, where P_s represents P_s and $a_{min}=\min(a_1, a_2)$. The glottal flow is given by $U=(2P_s/\rho)^{1/2}a_{min}\Theta(a_{min})$ using the air density constant ρ.

The parameter values were set as $m_1=0.125$ g, $m_2=0.025$ g, $k_1=80{,}000$ g s^{-2}, $k_2=8000$ g s^{-2}, $k_c=25{,}000$ g s^{-2}, $c_1=3k_1$, $c_2=3k_2$, $d_1=0.25$ cm, $d_2=0.05$ cm, $l=1.4$ cm and $\rho=0.00113$ g cm^{-2}, while the damping constants were set as $r_i=2\zeta(m_ik_i)^{1/2}$ using a damping ratio of $\zeta=0.05$. Dependence of the simulation results on the parameter setting is rather weak in the sense that essentially the same results can be obtained within a certain parameter range.

As the main parameters to control phonation, the P_s and the arytenoid distance x_0 were utilized. As the arytenoid distance defines the interval between the left and right vocal folds and thus determines the level of arytenoid adduction, we refer to x_0 as the adduction parameter. The adduction parameter was varied between 0.2 and –0.2. $x_0=0$ represents a neutral position in which the two vocal folds touch each other without adductive pressure. A negative adductive parameter represents situations in which the two vocal folds are firmly pressed against each other. A positive adductive parameter leaves a gap between the left and right vocal folds.

The output of the two-mass model is glottal flow (sometimes called 'acoustic flow' to be distinguished from the averaged tracheal airflow), which is a good approximation of the sound level of the source signal. Its spectral structure is a representation of vocal fold oscillation characteristics.

RESULTS

Morphology

Vocal fold length is positively correlated with body mass (Fig. 3). A scaling factor of 0.35 ($r^2=0.98$; Fig. 3), suggests that vocal fold length scales with body size almost with geometric similarity.

The vocal folds consist of muscular tissue, and a large mass of connective tissue covered with epithelium (Fig. 4). Fig. 5 shows the shape of one alligator's vocal fold during an inspiration. Cranially (Fig. 5A–E), the vocal folds are narrow and their dorsal aspect is almost shaped like a smaller fold sitting on the free edge. The vocal fold must have been actively deformed because this thin extension is not visible in the histological sections of the larynx (Fig. 4A,B).

In the cranial part, the vocal fold does not contain any muscle (Fig. 5A,B). Further caudal, muscles become part of the vocal fold

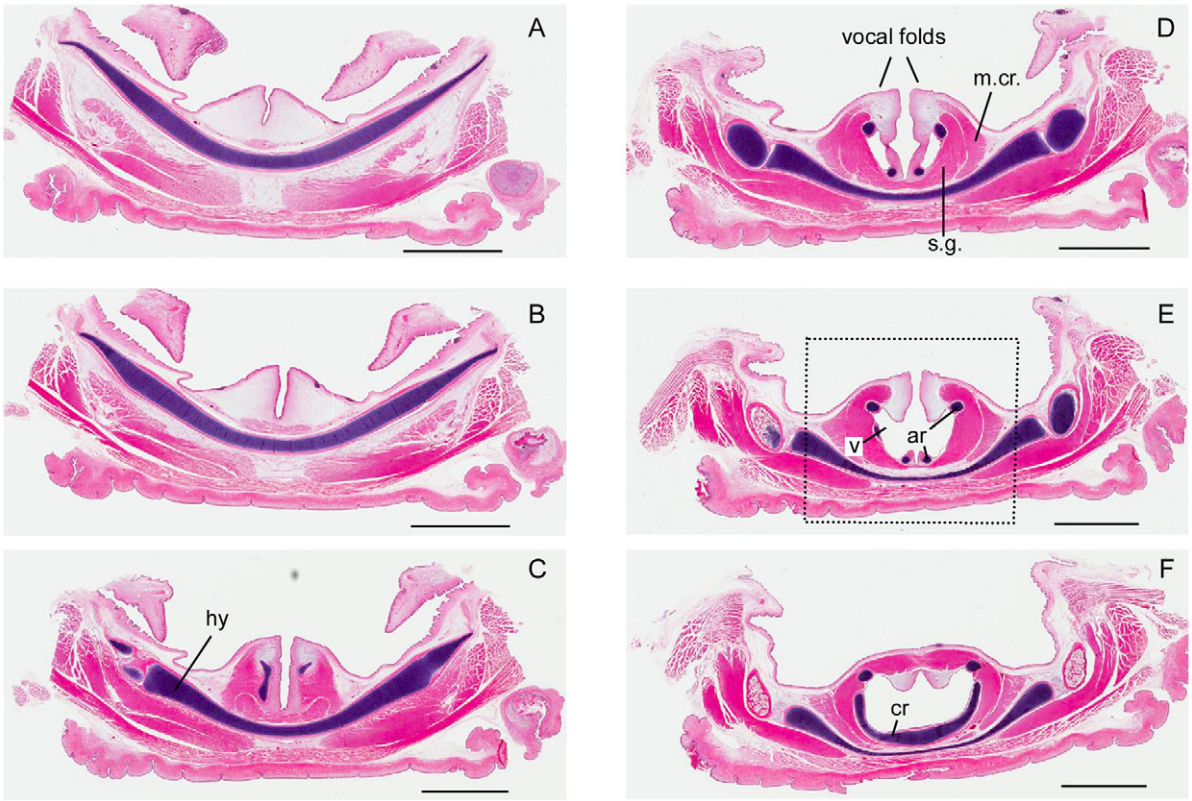

Fig. 4. Six sequential histological cross-sections through the larynx of a male 1.1 kg American alligator (hematoxylin and eosin stain), from cranial (A) to caudal (F) (~3 mm between subsequent levels). The section levels are comparable to the computer tomographic (CT) levels in Fig. 5. Levels in A and B correspond to Fig. 5B and C; however, note that the vocal folds in Fig. 5 are shaped differently. At this level the vocal folds are composed of extracellular matrix covered with epithelium. Intrinsic muscles visible in the caudal sections of the larynx (Fig. 3C–F) are responsible for the narrow shape in Fig. 5B and C. The musculus cricoarytenoideus (m.cr.) runs laterally from the medially positioned sphincter glottidis portion (s.g.) of the constrictor muscle (see Fig. 1B and C for comparison). Level in C corresponds to Fig. 5E or F. Note the processus vocalis of the arytenoid cartilage is sectioned in the left vocal fold (cf. Fig. 1A). Levels in D and E correspond to Fig. 5G–K. The dorsal and ventral branch of the arytneoid cartilage are cross-sectioned in both vocal folds. Level in F corresponds to Fig. 5L. hy, hyoid cartilage; cr, cricoid cartilage; ar, arytenoid cartilage. Scale bars are 5 mm. The dotted square in E corresponds to an outline of a similar area in Fig. 5G.

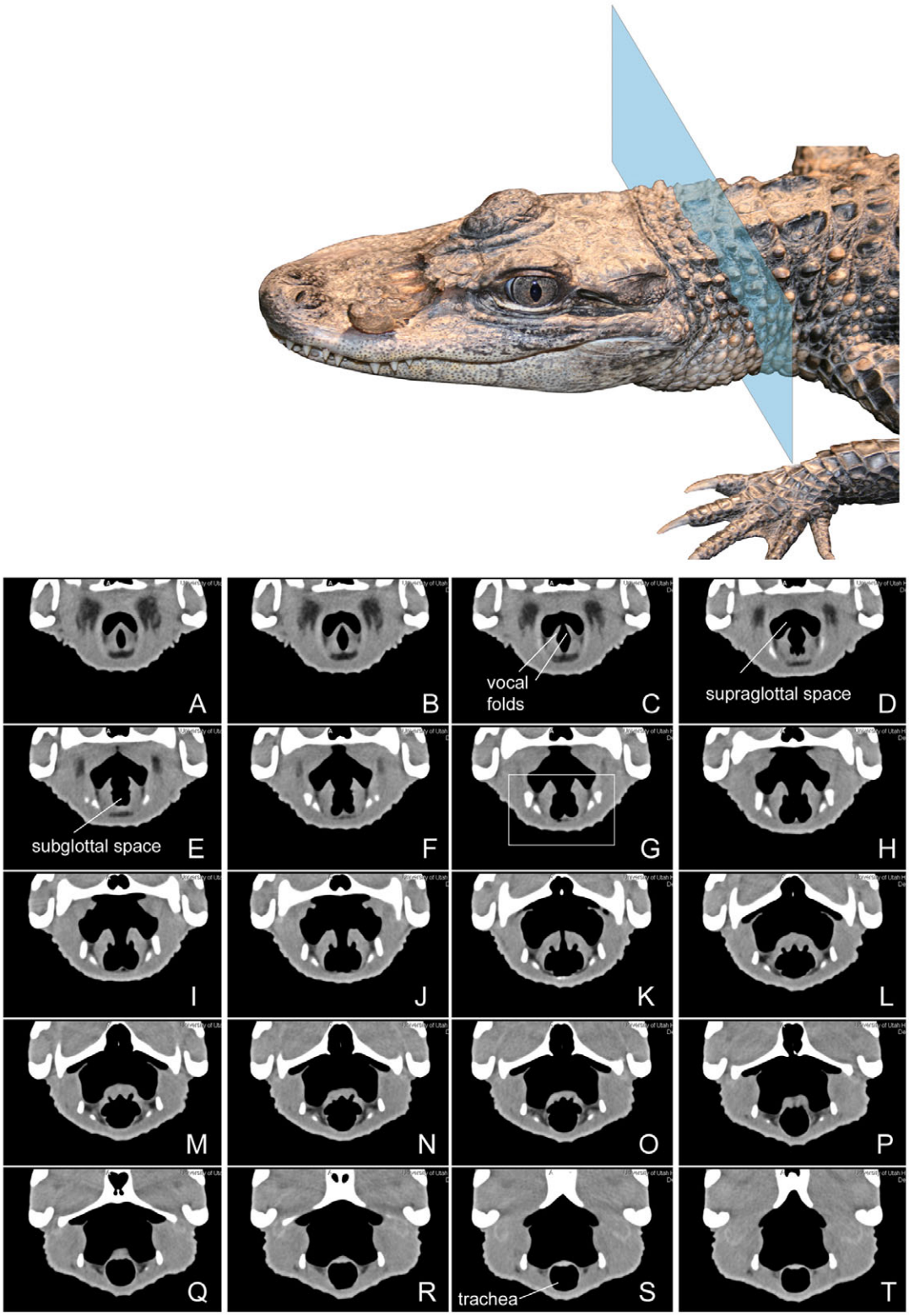

Fig. 5. (A–T) CT cross-sections from cranial to caudal (~1 mm distance in between two subsequent sections). One level is indicated by the plate in the upper image of an alligator. From C to K, the vocal folds are visible and the glottis is wide open. The animal is inspiring and the vocal folds are retracted laterally. Interestingly, the vocal folds show a thin shape, almost like thin membranes on the dorsal edge of the vocal folds. This membrane-like structure is not visible in the histological sections. Although we have little understanding of whether such a mechanism is used during phonation, this observation indicates that alligators can actively change the shape of their vocal folds into a certain prephonatory shape and/or position. The dotted square in G corresponds to an outline of a similar area in Fig. 4E.

and the arch-like arytenoid cartilages are also cross-sectioned (Fig. 4C,D). The *in vivo* shape (Fig. 5E–L) is similar as in the fixed material (Fig. 4C,F).

P_s during quiet respiration

Animals with a tracheal pressure transducer inserted through the glottis showed normal respiratory patterns. Mean ventilatory frequency during quiet respiration ranged between 0.4 and 6 breaths min^{-1}. The animal could inspire and hold the air for extended periods of time (Fig. 6A). P_s during the long holding phase ranged between 0.6 and 1.2 kPa. If the oral flap was tightly sealed, two valves in series, the larynx and/or the nostrils, could hold the air during the long holding phases. The nostrils were closed during the long holding phases but it is unclear whether

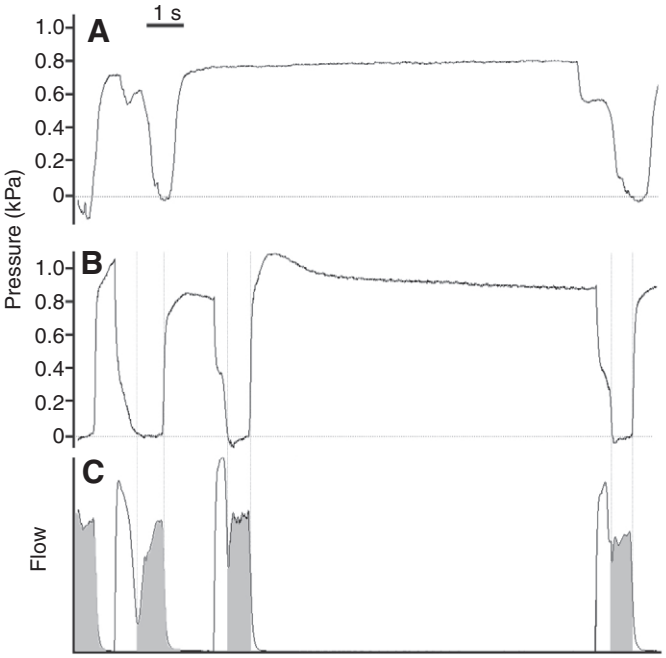

Fig. 6. Subglottal pressure (P_s) during quiet respiration recorded by two different procedures. (A) A pressure transducer was inserted through the glottis and placed in the trachea. The animal was basking below a red lamp. Two respiratory cycles are shown. (B and C) Same animal and similar situation. The pressure transducer and a flow thermistor were implanted percutaneously. The inspiratory phases are shaded. 0 kPa is ambient pressure.

they are the main valve 'holding the breath' or whether that function is performed by the larynx alone, and the nostrils just prevent water from entering the nasal cavity. Tracheal airflow was recorded in one animal (Fig. 6B,C). Maximum expiratory flow rates tend to exceed maximum inspiratory flow rates if the animal is resting. No flow was observed during the long holding phase.

It is interesting that the negative pressure during inspiration is very small (~0.1 kPa). Apparently the resistance provided by the nostriles and the glottis is very small during inspiration. During inspiration the nostriles are wide open. Visual inspection of the glottis confirmed that alligators were able to open the glottis widely during inspiration (at least one-half or two-thirds of the tracheal diameter).

P_s during contact call production

Calls are produced with an expiratory airflow. Mean call duration ranged between 49 and 974 ms in six individuals (Table 2). Prior to vocalization, P_s increased (Fig. 7A,B). During an ~200 ms period before voice onset, across six individuals, pressure rose to a mean of 2.5 kPa at phonation onset at rates between 0.7 and 2.4 kPa per 100 ms (Table 2). Prior to phonation onset no airflow was recorded (Fig. 7B). The glottis must be closed prior to phonation to allow P_s to increase until it reaches threshold pressure and air starts to be forced through the glottis (Fig. 7B), initiating vocal fold oscillation. Although the correlation between P_s and F_0 at the onset of a call is significant in five out of six individuals, variability is large (regression coefficients range between 0.3 and 0.91) (Table 3; Fig. 8).

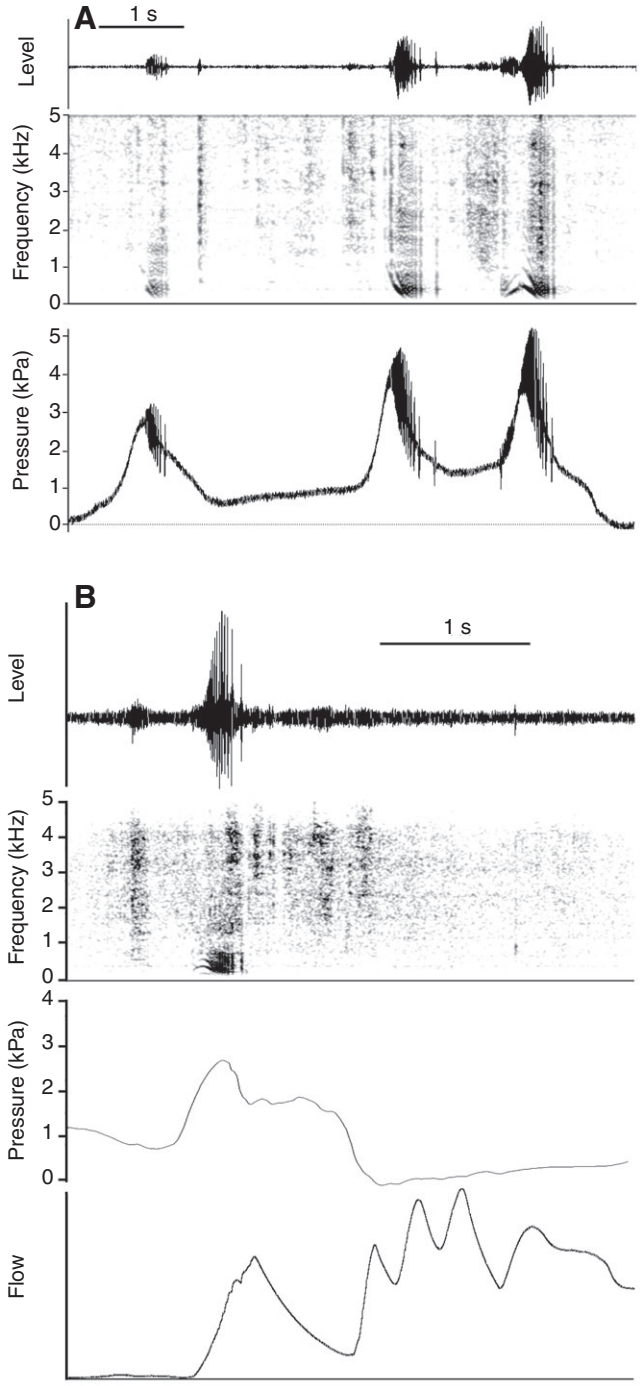

Fig. 7. (A) Waveform (top panel), spectrogram (middle panel) and P_s (bottom panel) during the production of two subsequent contact calls. P_s rises prior to call production for about 200 ms. In some calls maximum pressure coincides with phonation onset; in others it occurs shortly after the onset. (B) Waveform (first panel), spectrogram (second panel), P_s (third panel) and tracheal flow (fourth panel) during the production of a single contact call. P_s rises prior to call production for about 200 ms. In some calls maximum pressure coincides with phonation onset; in others it occurs shortly after the onset.

Phonation occurs during expiration. In one individual in which flow was recorded, we noted that pressure increased during the first half of the contact call and decreased during the second half of the vocalization while flow continued to rise (Fig. 7B), suggesting that

Table 3. Correlations between F_0 and P_s at call onset and at the point of maximum F_0

ID no.	F_0 *versus* P_s onset	F_0 *versus* P_s max.	F_0 *versus* P_s end
736	***r*=0.92**	***r*=0.95**	*r*=0.33
(*N*=22)	*P*<0.001	*P*<0.001	*P*=0.12
741	***r*=0.89**	***r*=0.73**	***r*=0.45**
(*N*=22)	*P*<0.001	*P*<0.001	*P*=0.035
738	***r*=0.71**	***r*=0.71**	***r*=0.88**
(*N*=22)	*P*<0.001	*P*=0.03	*P*<0.001
737	***r*=0.55**	***r*=0.54**	*r*=0.15
(*N*=22)	*P*=0.01	*P*=0.02	*P*=0.50
749	***r*=0.96**	***r*=0.78**	*r*=0.24
(*N*=12)	*P*<0.001	*P*<0.01	*P*=0.43
742	*r*=0.46	*r*=0.05	*r*=0.55
(*N*=4)	*P*=0.69	*P*=0.96	*P*=0.45

Significant relationships are shown in bold. P_s onset, subglottal pressure at call onset; P_s max., subglottal pressure at maximum F_0 in the call; P_s end, subglottal pressure at the end of a call.

the animal begins to abduct the glottis at least by about the middle of the vocalization (maybe earlier) thereby changing the resistance in the respiratory tract. An identical pattern was observed in two other growl vocalizations. The pressure–flow relationship can be explained by Ohm's law according to which flow rate is determined by the ratio between P_s and resistance. If P_s decreases and airflow continues to increase, then resistance must also decrease. The glottis is the most likely candidate to serve as a valve inside the vocal tract, because the mouth flap is closed, the nostrils are wide open and no other constricting structure is found in the nasal and pharyngeal vocal tract.

The call can be followed by gular pumps during which the glottis can remain open. The rapid flow changes in the second half of Fig. 7B, which are mirrored in the pressure signal only by small variations, were associated with gular pumps during which the nostrils were closed.

In some calls the onset of phonation coincided with the maximum P_s level. In others, P_s continued to increase after phonation onset (Fig. 7A, second call). The maximum P_s at call onset across six individuals was 2.8 kPa (Table 2). The correlation between P_s and F_0 at the time point of maximum P_s was significant in five individuals (regression coefficients range between 0.29 and 0.89) (Table 3; Fig. 8).

P_s decreased toward the end of the call to a mean of 1.3 kPa at call offset (Table 2). The correlation between P_s and F_0 at the end of a call was significant in two out of six individuals (Table 3).

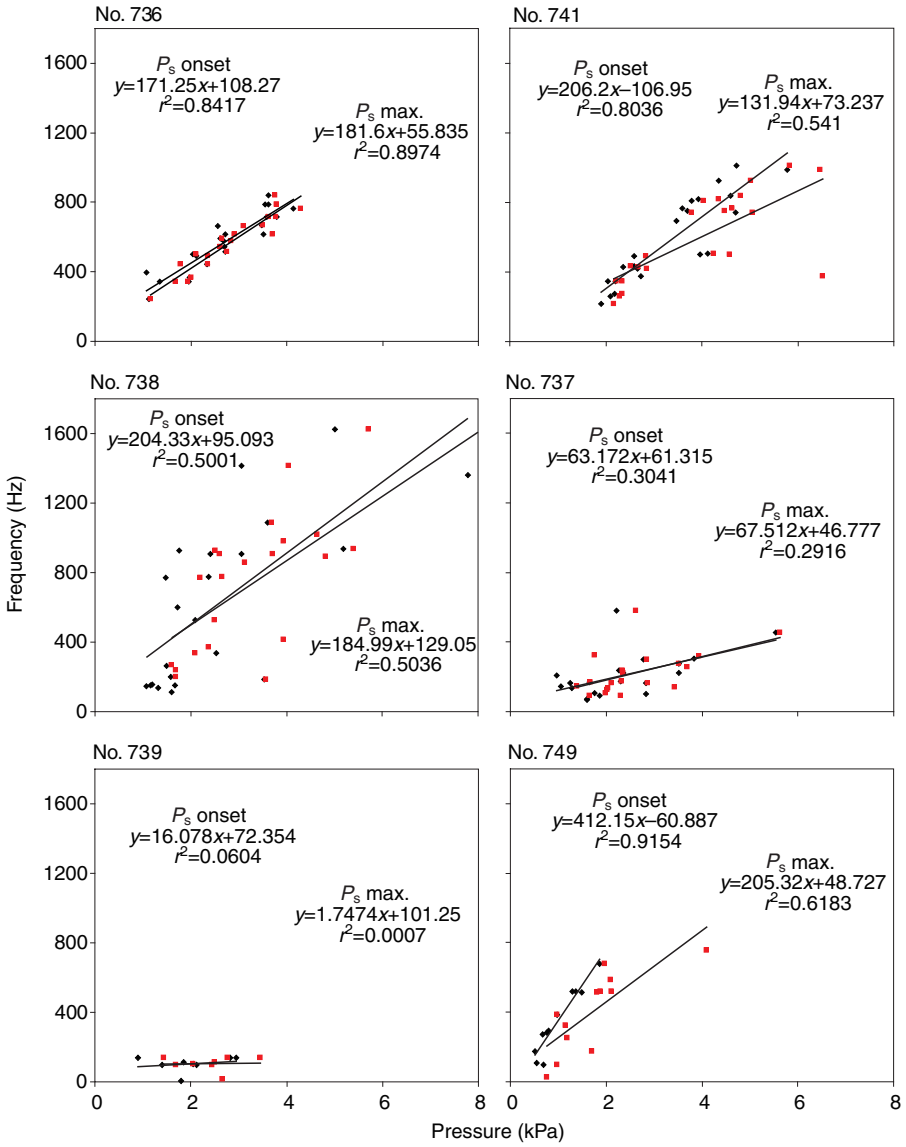

Fig. 8. Relationship between P_s and fundamental frequency (F_0) at call onset (P_s onset, black circles) and at the position of the maximum F_0 (P_s max., red circles) in six alligators.

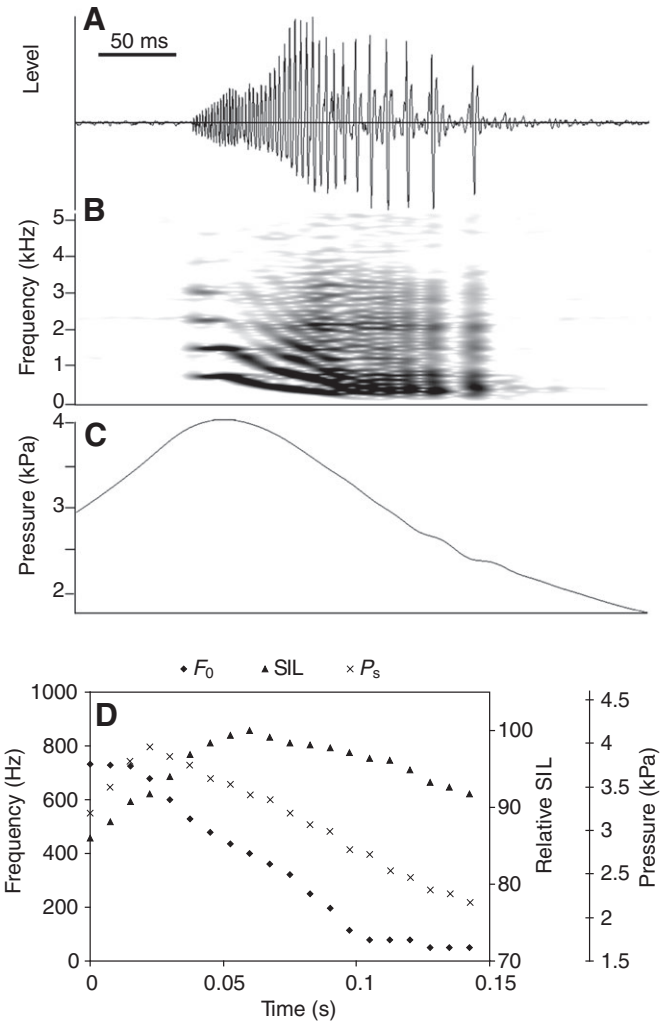

Fig. 9. Waveform (A), spectrogram (B) and P_s (C) of a contact call. Note that here the pressure signal was down-sampled at 120 Hz (in contrast to Fig. 5 and 6 where unfiltered pressure signals are shown). (D) Three parameters (F_0, P_S; relative sound intensity level, SIL) measured in 10 ms intervals in the call shown in A and B.

The inconsistent relationship between F_0, P_s and SIL can also be seen in the contours of all three parameters. F_0 reached a maximum early in a call and decreased toward the end of a call (Fig. 9). P_s also peaked early in a call (Fig. 9C), while SIL reached a maximum later in the call (Fig. 9A,D). The time point at which F_0, P_s and SIL reached a maximum was on average 11.1%, 24.2% and 55.7%, respectively, into a call (Table 4). Fig. 10A–C shows data for all calls of one individual including the respective 2nd degree polynominal models. The average models of the contours for F_0, P_s and SIL for six individuals are shown in Fig. 10D.

The effect of P_s on F_0 modulation is limited. Large values can therefore be seen as an indication that additional mechanisms contribute to modulate frequency. The mean F_0 change per 1 kPa pressure change in alligator calls ranged between 250 and 512 Hz kPa^{-1} (Table 5) suggesting an active laryngeal mechanism must be involved.

Computer simulation of a contact call

The computer simulation of a frequency-modulated call utilizing P_s and vocal fold adduction as the only control parameters was successful. In 200 ms simulations the frequency modulation from start to end of the simulation ranged between 950 and 200 Hz (Fig. 11). Two factors are responsible for the frequency modulation throughout the simulation: while the adduction parameter continuously increased, P_s continuously decreased from 3.5 to 1.5 kPa (Fig. 11). Frequency modulation and high initial pressure agree well with the frequency modulation in an alligator call. P_s alone can modulate F_0, but the effect is small (Fig. 12A). For example, at a constant adduction parameter of x_0=0 and a P_s change from 3.5 to 1.5 kPa, a frequency modulation of only 190 Hz (or 95 Hz kPa^{-1}) was achieved in the simulation. A combination of variable adduction and P_s can achieve frequency modulations of more thn 300 Hz kPa^{-1} (Fig. 12B).

DISCUSSION

Sources of acoustic variation

Although both male and female alligators produce loud low-frequency ‘bellow’ vocalizations during the mating season, some components of the vocal display are sexually dimorphic. A low frequency component, described by Vliet as a ‘subaudible component’, is not produced by females and various temporal parameters also differ between males and females (Vliet, 1989). Alligator vocal fold length does not differ between sexes and scales isometrically with body size in both sexes. Sexually dimorphic vocal behavior in mammals, birds and frogs arises from differences in central neural control (Bass, 1992; Wade and Arnold, 2004) and differences in the functional morphology of peripheral organs [e.g. humans (Titze, 1989b); zebra finch (*Taeniopygia guttata*) (Riede et al., 2010a); Tungara frogs (*Physalaemus pustulosus*) (Ryan and Drewes, 1990)]. Besides vocal fold length, other important factors responsible for sexually dimorphic vocal characteristics include viscoelastic properties of vocal folds (e.g. Riede et al., 2010b) or interactions between the sound source and the vocal tract filter (Titze

Table 4. Model parameters for normalized call duration against F_0, P_s and SIL

	F_0				P_s				SIL			
ID no.	*a*	*b*	*c*	*Z* (%)	*a*	*b*	*c*	*Z* (%)	*a*	*b*	*c*	*Z* (%)
741	0.00005	–0.7914	93.48	3.2±5.9	–0.0049	0.1619	88.95	16.7±13.7	–0.0048	0.557	82.45	65.3±12.3
738	–0.0022	–0.529	89.96	6.99±10.5	–0.0051	0.235	84.86	18.3±23.3	–0.0044	0.479	85.98	41.5±14.4
749	0.0014	–0.7381	98.66	12.6±21.6	–0.0065	0.622	82.34	50.2±33.2	–0.003	0.417	83.29	67.6±14.4
742	–0.0043	–0.1399	86.6	18.9±14.7	–0.0038	0.124	91.3	21.8±22.5	–0.0019	0.205	92.98	58.3±18.0
736	0.0025	–0.9219	98.2	2.1±5.9	–0.0034	0.017	93.53	14.86±12.6	–0.003	0.2924	92.1	40.9±12.0
737	–0.0033	–0.055	85.75	23.1±17.2	–0.0016	0.1643	79.4	23.4±30.5	–0.0022	0.246	87.9	60.4±20.6

Data were fitted with a 2nd degree polynomial model ($y=ax^2+bx+c$). The constants *a*, *b* and *c* are shown as means averaged over an individual’s calls. *Z* is the zero (mean ± s.d.) of the models calculated for each call. The zero indicates the relative position of maximum for F_0, P_s and SIL within a call.

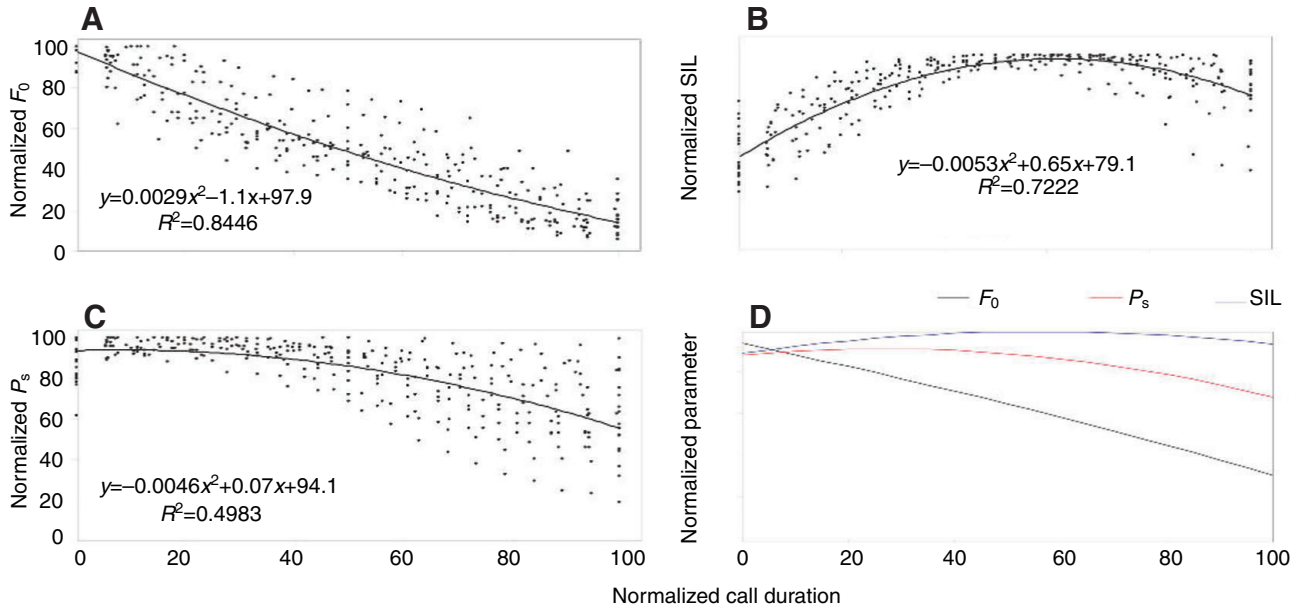

Fig. 10. Relationship between normalized call duration and three normalized parameters (F_0, P_s and SIL). (A–C) Example data for individual 741. Data were fitted by a 2nd degree polynomial model. (D) Polynomial models for three parameters based on averaged data from six individuals (see Table 3).

et al., 2008). None of these mechanisms have been investigated in alligators.

We found that P_s alone cannot explain differences in F_0 or frequency modulations. One or more intrinsic laryngeal motor patterns are necessary to account for frequency differences and frequency modulation. The results of the modeling approach imply that combined tuning of both the P_s and the arytenoid positioning (adduction) can produce a frequency modulation with similar magnitude to that in alligator calls. In the simulation, the vocal folds were continuously abducted and P_s was decreased. For a small adduction parameter, the left and right vocal folds are located close to each other (i.e. arytenoid distance is small or vocal folds are pressed against each other), enhancing the occurrence of vocal fold collision. As the cycle time of the vocal folds is also shortened by this small adduction parameter, the vocal fold oscillations are strongly accelerated to produce a high frequency call. In contrast, a large adduction parameter has the opposite effect; it slows down the vocal fold oscillations and causes the F_0 to decrease.

In alligators, expiration is driven by the activity of the abdominal muscle sheet (m. transversus abdominis, m. rectus abdominis) and intercostal musculature (Naifeh et al., 1970; Gans and Clark, 1976; Farmer and Carrier, 2000a). Elastic recoil of the lung tissue is unlikely to add to the expiratory pressure because lung compliance is large (Perry and Duncker, 1980). We found that P_s ranges between 0.4 and 8 kPa during contact call production in juvenile alligators (Table 2). This range overlaps greatly with what is found in mammals [humans (Bouhuys et al., 1969; Holmberg et al., 1988; Plant and Younger, 2000; Plant et al., 2004); bats (Fattu and Suthers, 1981)], in frogs (Martin, 1972) and in birds (Riede et al., 2010a). If P_s increases while vocal fold tension remains constant, vocal folds will be pushed laterally a little further, decreasing the length/amplitude ratio. The wider excursion will strain the vocal fold more and tension will be greater at maximum amplitude, leading to a small increase in oscillation rate and, consequently, in F_0. The pressure effect on frequency is highly dependent on tissue tension. It ranges between 5 and 70 Hz per 1 kPa P_s change in humans (Titze, 1989a; Titze, 1988a), and between 20 and 50 Hz per 1 kPa P_s change in zebra finches (Riede et al., 2010a). Our current computer simulation suggests a value of 80 Hz per 1 kPa P_s change.

Increasing tension by stretching the vocal fold (in the larynx) or labia (in the syrinx) can change frequency much more dramatically than P_s changes alone (Hollien, 1960; Hirano et al., 1969; Nishizawa et al., 1988; Riede et al., 2010a). The effect of adduction on F_0 and on vocal intensity is well known from studies in humans and excised mammalian larynx experiments (e.g. Hillman et al., 1990; Titze, 1988a; Alipour and Scherer, 2007). The vocal fold model suggests that frequency modulations of several hundred Hertz can be achieved in a concerted modulation of pressure and adduction. A better understanding of the magnitude of adduction in the alligator larynx would allow the simulation results to be tested. Anecdotal observations suggest that laryngeal adduction can be large in alligators: the insertion of the small pressure transducer through the glottis was very difficult in the tightly closed glottis and usually had to await the next inspiration. An important variable also missing is glottal airflow. The anecdotal observation in one animal when subgottal pressure decreased while glottal flow continued to increase indicated a change in adduction during vocalization (Fig. 7B). Simultaneous glottal flow and P_s would also improve the computer modeling.

Table 5. Mean (±s.d.) fundamental frequency change per 1 kPa subglottal pressure change

ID no.	Frequency change per 1 kPa pressure change (Hz kPa^{-1})
736 (N=14)	393±86
741 (N=15)	280±106
738 (N=16)	512±259
737 (N=10)	250±160
749 (N=5)	373±122
742 (N=3)	263±235

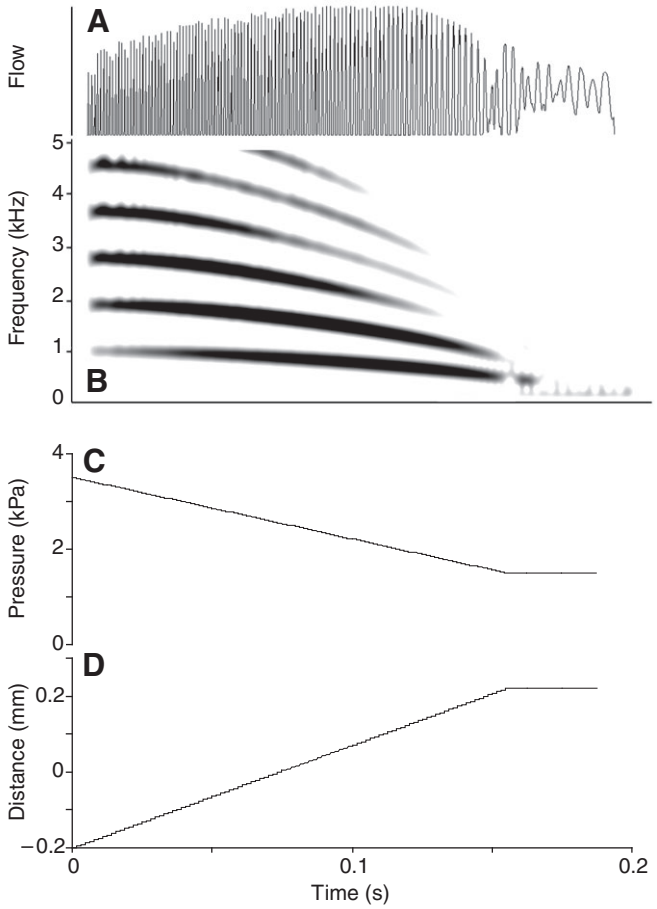

Fig. 11. Source signal (glottal flow) (A), spectrogram (B), P_s (C) and vocal fold adduction (D) during call simulation with P_s and adduction as the only variables. P_s was decreased from 3.5 to 1.5 kPa, whereas the adduction parameter was changed from –0.2 to 0.2 cm. F_0 decreased from ~900 Hz to ~200 Hz.

A narrowing of the upper edge of the vocal fold may support the frequency modulation. Anatomical studies suggest that the upper and lower aspect of the vocal fold can be independently adducted (Henle, 1839; Söller, 1931). CT images confirmed that during quiet respiration an alligator was able to change vocal fold shape in the expected pattern. Computer models simulating a narrow vocal fold edge that extends like a small fold on the free edge of the normal vocal fold show that this can indeed contribute to extension of the frequency range (Tokuda et al., 2007).

A primitive feature of the alligator larynx

The physiology of voice production has been investigated in mammals (e.g. Jürgens, 2002; Ludlow, 2005; Suthers and Fattu, 1982; Titze, 2000), birds (e.g. Suthers and Zollinger, 2004; Goller and Cooper, 2004; Riede and Goller, 2010), amphibians (e.g. Martin and Gans, 1972) and fish (Bass et al., 2008), but data were missing in reptiles (Gans and Maderson, 1973). Three conditions are necessary (i.e. critical) and sufficient for phonation by flow-induced tissue vibrations in a larynx – a concept summarized as the myoelastic–aerodynamic theory of voice production (van den Berg, 1958; Titze, 2006). First, the vocal folds must be positioned close to the midline constricting the airway (adduction). Across vertebrates possessing a larynx, abduction and adduction are achieved by various forms of constrictor muscles. Alligators possess a dilator and a constrictor muscle, the latter consisting of two parts possibly achieving a differentiated adduction between the dorsal and ventral parts of the glottis. Second, an aerodynamic driving force (P_s) causes air to flow by the vocal folds. Third, vocal fold mechanical properties determine oscillation rate and amplitude. Elongation and shortening is an active mechanism that determines the effective tension and shape of vocal folds. A tensor mechanism is very important in mammals (Hollien, 1960; Titze, 1991) and many frogs (Trewavas, 1933; Martin, 1972), but has not been identified in alligators or other reptiles (Fraher et al., 2010).

Tension control of vocal folds is possible in frogs and mammals. In frogs, it is achieved by the posterior portion of the constrictor muscle, which is continuous with the vocal fold, allowing it to apply strain to the vocal fold (Trewavas, 1933; Martin, 1972), except in Bufonidae where this muscle has supposedly been lost (Trewavas, 1933, Martin, 1972). In mammals, vocal fold length changes are effected by an interplay between the cricothyroid muscle and the thyroarytenoid muscle (Hollien, 1960; Hirano et al., 1969). The consequence of an ability not only to abduct and adduct vocal folds but also to elongate and shorten them at will is twofold. First, the F_0 range can be enormously extended. In a first approximation, vocal fold behavior in mammals compares to that of a string because tension determines the oscillation rate determining F_0. The way to increase tension in vocal folds is to elongate them. This seems counter-intuitive because longer strings/vocal folds should posses a lower resonance frequency than shorter ones. Viscoelastic properties of vocal fold tissue, however, specifically the exponential increase in tissue stress under stretch, overcomes the frequency decrease caused by the length increase (e.g. Riede, 2010).

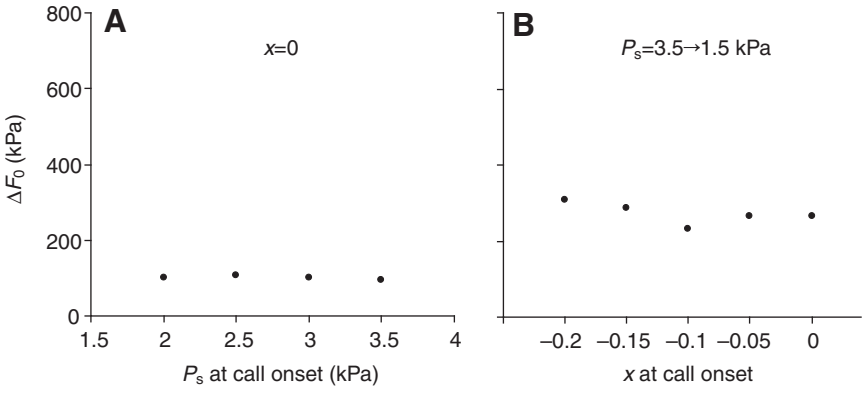

Fig. 12. The effect of P_s and vocal fold adduction (x) on F_0 modulation (ΔF_0). (A) Vocal fold adduction was kept constant while P_s was changed from the initial pressure to 1.5 kPa at the end of the simulation (200 ms). (B) Both parameters were varied. In all five simulations P_s was changed from 3.5 to 1.5 kPa, and adduction was varied between the initial value at onset and 0.2 at the end of the simulation.

Second, a controlled tensor mechanism allows control of F_0 modulation. The step towards a direct and rigorous control of frequency has been identified in mammals. Mammalian vocal folds are positioned between two anchor points (ventrally the thyroid cartilage, dorsally the arytenoid cartilage). The cricothyroid muscle and the thyroarytenoid muscle determine the length and thickness of the vocal fold in a finely tuned interplay (e.g. Hast et al., 1974; West and Larson, 1993; Jürgens, 2002), allowing precise frequency control. In songbirds a similar step towards direct and rigorous frequency control has been identified. In songbirds, tension regulation of labia is the main parameter to extend the F_0 range and produce a highly stereotypic frequency pattern including frequency modulation. Pairs of labia inside the syrinx are set into vibration by a passing airflow (Goller and Larson, 1997), and syringeal muscle activity alters the tension of the labia to achieve stereotypic oscillation rates (Goller and Suthers, 1996), extending the frequency range beyond what would be possible by pressure changes alone (Riede et al., 2010a); unlike in suboscines, where a more pressure-driven frequency control exists (Amador et al., 2008).

More experimentation will be necessary in alligators to determine the contribution of intrinsic larynx muscles to frequency control. Furthermore, once sound is produced it must travel from the larynx through the vocal tract (oral, pharyngeal and nasal cavity) before it can radiate from the mouth, nares and/or skin. As vocalization often occurs while the animal is submerged and sound could propagate underwater (Fine et al., 2004), understanding sound properties in the vocal tract and of radiators is also very important. Also of interest is the very consistent pulse tone pattern at the end of contact calls. Pulse tone phonation is well known in mammals (Riede and Zuberbühler, 2003), birds (Jensen et al., 2007) and frogs (Martin, 1972). Remarkable in alligators is the relatively high sound amplitude during pulse tone phonation, while P_s continues to decrease.

ACKNOWLEDGEMENTS

We are grateful to Franz Goller and Michael Fine for discussions and important comments on an earlier version of the manuscript and to Kent Sanders for the CT data. Funding for this work was provided in part by NIH grants R01 DC008612 and R01DC006876 and NSF grant IOS 0810973. Tissue was provided through the Alligator Tissue Bank at UC Irvine (NSF grant IOS 0922756 to Jim Hicks). Deposited in PMC for immediate release.

OPEN ACCESS

REFERENCES

Alipour, F. and Scherer, R. C. (2007). On pressure-frequency relations in the excised larynx. *J. Acoust. Soc. Am.* **122**, 2296-2305.
Amador, A., Goller, F. and Mindlin, G. B. (2008). Frequency modulation during song in a suboscine does not require vocal muscles. *J. Neurophysiol.* **99**, 2383-2389.
Bass, A. (1992). Dimorphic male brains and alternative reproductive tactics in a vocalizing fish. *Trends Neurosci.* **15**, 139-144.
Bass, A. H., Gilland, E. H. and Baker, R. (2008). Evolutionary origins for social vocalization in a vertebrate hindbrain–spinal compartment. *Science* **321**, 417-421.
Boersma, P. and Weenink, D. (2008). Praat: doing phonetics by computer [computer program]. Version 5.0.41, retrieved November 2008 from http://www.praat.org/.
Bouhuys, A., Mead, J., Proctor, D. F. and Stevens, K. N. (1968). Pressure-flow events during singing. *Ann. NY Acad. Sci.* **155**, 165-176.
Claessens, L. P. (2009). A Cineradiographic study of lung ventilation in *Alligator mississippiensis*. *J. Exp. Zool.* **311A**, 563-585.
Cranen, B. and Boves, L. (1985). Pressure measurements during speech production using semiconductor miniature pressure transducer: Impact on models for speech production. *J. Acoust. Soc. Am.* **77**, 1543-1551.
Farmer, C. G. and Carrier, D. R. (2000a). Pelvic aspiration in the American alligator (*Alligator mississippiensis*). *J. Exp. Biol.* **203**, 1679-1687.
Farmer, C. G. and Carrier, D. R. (2000b). Ventilation and gas exchange during treadmill locomotion in the American alligator (*Alligator mississippiensis*). *J. Exp. Biol.* **203**, 1671-1678.
Farmer, C. G. and Sanders, K. (2010). Unidirectional airflow in the lungs of alligators. *Science* **327**, 338-340.
Fattu, J. M. and Suthers, R. A. (1981). Subglottic pressure and the control of phonation by the echolocating bat, *Eptesicus*. *J. Comp. Physiol.* **143**, 465-475.
Ferguson, M. W. J. (1981). The structure and development of the palate in *Alligator mississippiensis*. *Archs Oral Biol.* **26**, 427-443.
Fine, M. L., Schrinel, J. and Cameron, T. M. (2004). The effect of loading on disturbance sounds of the Atlantic croaker *Micropogonius undulatus*: air vs. water. *J. Acoust. Soc. Amer.* **116**, 1271-1275.
Flanagan, J. L. (1972). *Speech Analysis, Synthesis and Perception*. Berlin: Springer.
Fraher, J., Davenport, J., Fitzgerald, E., McLaughli, P., Doyle, T., Harman, L. and Cuffe, T. (2010). Opening and closing mechanisms of the leatherback sea turtle larynx: a crucial role for the tongue. *J. Exp. Biol.* **213**, 4137-4145.
Gans, C. and Clark, B. (1976). Studies on ventilation of *Caiman crocodilus* (Crocodilia, Reptilia). *Respir. Physiol.* **26**, 285-301.
Gans, C. and Maderson, P. F. A. (1973). Sound producing mechanisms in recent reptiles: review and comment. *American Zoologist* **13**, 1195-1203.
Goller, F. and Cooper, B. G. (2004). Peripheral motor dynamics of song production in the zebra finch. *Ann. NY Acad. Sci.* **1016**, 130-152.
Goller, F. and Larsen, O. N. (1997). A new mechanism of sound generation in songbirds. *Proc. Natl. Acad. Sci. USA* **94**, 14787-14791.
Goller, F. and Suthers, R. A. (1996). Role of syringeal muscles in controlling the phonology of bird song. *J. Neurophysiol.* **76**, 287-300.
Göppert, E. (1899). Der Kehlkopf der Amphibien und Reptilien. II. Theil. Reptilien. *Morphologische Jahrbücher* **28**, 1-27.
Göppert, E. (1937). Atmungssystem. I. Kehlkopf und Trachea. In *Handbuch der vergleichenden Anatomied er Wirbeltiere*, Vol. 3 (ed. L. Bolk, E. Göppert, E. Kallius and W. Lubosch), pp. 797-866. Berlin: Urban and Schwarzenberg.
Hast, M. H., Fischer, J. M., Wetzel, A. B. and Thompson, V. E. (1974). Cortical motor representation of the laryngeal muscles in *Macaca mulatta*. *Brain Res.* **73**, 229-240.
Henle, F. G. J. (1839). *Vergleichend-anatomische Beschreibung des Kehlkopfes mit besonderer Berücksichtigung des Kehlkopfes der Reptilien.* Leipzig: Verlag von Leopold Voss.
Herzog, H. A. and Burghardt, G. M. (1977). Vocalizations in juvenile crocodilians. *Z. Tierpsychol.* **44**, 294-304.
Hillman, R. E., Holmberg, E. B., Perkell, J. S., Walsh, M. and Vaughan, C. (1990). Phonatory function associated with hyperfunctionally related vocal fold lesions. *J. Voice* **4**, 52-63.
Hirano, M., Ohala, J. and Vennard, W. (1969). The function of laryngeal muscles in regulating fundamental frequency and intensity of phonation. *J. Speech Hear. Res.* **12**, 616-628.
Hollien, H. (1960). Vocal pitch variation related to changes in vocal fold length. *J. Speech Hear. Res.* **3**, 150-156.
Holmberg, E., Hillman, R. and Perkell, J. (1988). Glottal airflow and transglottal air pressure measurements for male and female speakers in soft, normal and loud voice. *J. Acoust. Soc. Am.* **84**, 511-529.
Ishizaka, K., and Flanagan, J. L. (1972). Synthesis of voiced sounds from a two-mass model of the vocal cords. *Bell Syst. Tech. J.* **51**, 1233-1268.
Jensen, K. K., Cooper, B. G., Larsen, O. N. and Goller F. (2007). Songbirds use pulse tone register in two voices to generate low-frequency sound. *Proc. R. Soc. B* **274**, 2703-2710.
Jiang, J. J. and Titze, I. R. (1994). Measurement of vocal fold intraglottal pressure and impact stress. *J. Voice* **8**, 132-144.
Jürgens, U. (2002). Neural pathways underlying vocal control. *Neurosci. Behav. Rev.* **26**, 235-258.
Ludlow, C. L. (2005). Central nervous system control of the laryngeal muscles in humans. *Resp. Physiol. Neurobiol.* **147**, 205-222.
Martin, W. F. (1972). Evolution of vocalization in the genus *Bufo*. In *Evolution in the Genus Bufo* (ed. W. F. Blair), pp. 279-309. Austin: University of Texas Press.
Martin, W. F. and Gans, C. (1972). Muscular control of the vocal tract during release signalling in the toad *Bufo valliceps*. *J. Morph* **137**, 1-27.
Müller, J. (1839). *Compensation der physischen Kräfte am menschlichen Stimmorgan,* pp. 1-54. Berlin, Hirschwald Verlag.
Naifeh, K. H., Huggins, S. E. and Hoff, H. E. (1970). The nature of the nonventilatory period in crocodilian respiration. *Respir. Physiol.* **10**, 338-348.
Negus, C. (1949). *The Comparative Anatomy and Physiology of the Larynx*. New York: Grune and Stratton.
Nishizawa, N., Sawashima, M. and Yonemoto, K. (1988). Vocal fold length in vocal pitch change. In V*ocal physiology: Voice Production, Mechanisms and Functions*. (ed. O. Fujimura), pp. 75-82. New York: Raven Press.
Owerkowicz, T., Farmer, C. G., Hicks, J. W. and Brainerd, E. L. (1999). Contribution of gular pumping to lung ventilation in monitor lizards. *Science* **284**, 1661-1663.
Perry, S. F. and Duncker, H. R. (1980). Interrelationship of static mechanical factors and anatomical structure in lung evolution. *J. Comp. Physiol. B* **138**, 321-334.
Plant, R. L. and Younger, R. M. (2000). The interrelationship of subglottic air pressure, fundamental frequency, and vocal intensity during speech. *J. Voice* **14**, 170-177.
Plant, R. L., Freed, G. L. and Plant, R. E. (2004). Direct measurement of onset and offset phonation threshold pressure in normal subjects. *J. Acoust. Soc. Am.* **116**, 3640-3646.
Reese, A. M. (1915). *The Alligator and its Allies.* New York: The Knickerbocker Press.
Reese, A. M. (1945). The laryngeal region of *Alligator mississippiensis*. *Anatomical Record* **92**, 273-277.
Riede, T. (2010). Elasticity and stress relaxation of rhesus monkey (*Macaca mulatta*) vocal folds. *J. Exp. Biol.* **213**, 2924-2932.

Riede, T. and Goller, F. (2010). Peripheral mechanisms for vocal production in birds – differences and similarities to human speech and singing. *Brain Lang.* **115**, 69-80.
Riede, T. and Zuberbühler, K. (2003). Pulse register phonation in Diana monkey alarm calls. *J. Acoust. Soc. Am.* **113**, 2919-2926.
Riede, T., Suthers, R. A., Fletcher, N. H. and Blevins, W. (2006). Songbirds tune their vocal tract to the fundamental frequency of their song. *Proc. Natl. Acad. Sci. USA* **103**, 5543-5548.
Riede, T., Tokuda, I. T., Munger, J. B. and Thomson, S. L. (2008). Mammalian laryngeal air sacs add variability to the vocal tract impedance: physical and computational modeling. *J. Acoust. Soc. Am.* **124**, 634-647.
Riede, T., Fisher, J. H. and Goller, F. (2010a). Sexual dimorphism of the sound generating labia and the cartilaginous framework in the syrinx of zebra finches. *PLoS One* **5**, e11368.
Riede, T., Lingle, S., Hunter, E. H. and Titze, I. R. (2010b). Cervids with different vocal behavior demonstrate different visco-elastic properties of their vocal folds. *J. Morphol.* **271**, 1-11.
Ryan, M. J. and Drewes, R. C. (1990). Vocal morphology of the *Physalaemus pustulosus* species group (family Leptodactylidae): morphological response to sexual selection for complex calls. *Biol. J. Linn. Soc. Lond.* **40**, 37-52.
Söller, L. (1931). Über den Aufbau und die Entwicklung des Kehlkopfes bei Krokodilen und Marsupialiern. *Morph. Jahrbuch.* **68**, 541-593.
Steinecke, I. and Herzel, H. (1995). Bifurcations in an asymmetric vocal fold model. *J. Acoust. Soc. Am.* **97**, 1874-1884.
Suthers, R. A. and Fattu J. M. (1982). Selective laryngeal neurotomy and the control of phonation by the echolocating bat, *Eptesicus. J. Comp. Physiol.* **145**, 529-537.
Suthers, R. A. and Zollinger, S. A. (2004). Producing song: the vocal apparatus. *Ann. NY Acad. Sci.* **1016**, 109-129.
Titze, I. R. (1988a). Regulation of vocal power and efficiency by subglottal pressure and glottal width. In *Vocal Physiology* (ed. O. Fujimura). New York: Raven Press.
Titze, I. R. (1988b). The physics of small-amplitude oscillation of the vocal folds. *J. Acoust. Soc. Am.* **83**, 1536-1552.
Titze, I. R. (1989a). On the relation between subglottal pressure and fundamental frequency in phonation. *J. Acoust. Soc. Am.* **85**, 901-906.
Titze I. R. (1989b). Physiologic and acoustic differences between male and female voices. *J. Acoust. Soc. Am.* **85**, 1699-1707.
Titze, I. R. (1991). Mechanisms underlying the control of fundamental frequency. In *Vocal Fold Physiology: Acoustic Perceptual and Physiological Aspects of Voice Mechanisms* (ed. J. Gauffin and B. Hammarberg), pp. 129-138. San Diego: Singular Publishing Group, Inc.
Titze, I. R. (2000). *Principles of Voice Production*. Salt Lake City, Utah: National Center for Voice and Speech.
Titze, I. R. (2006). *The Myoelastic Aerodynamic Theory of Phonation*. Denver: The National Center for Voice and Speech.
Titze, I. R., Riede, T. and Popollo, P. (2008). Vocal exercises to determine nonlinear source-filter interaction. *J. Acoust. Soc. Am.* **123**, 1902-1915.
Tokuda, I. T., Horáek, J., Švec, J. G. and Herzel, H. (2007). Comparison of biomechanical modeling of register transitions and voice instabilities with excised larynx experiments. *J. Acoust. Soc. Am.* **122**, 519-531.
Tokuda I. T., Zemke, M., Kob, M. and Herzel, H. (2010). Biomechanical modeling of register transitions and the role of vocal tract resonators *J. Acoust. Soc. Am.* **127**, 1528-1536.
Trewavas, E. (1933). The hyoid and larynx of the Anura. *Phil. Trans. R. Soc., London* **222**, 401-527.
Van den Berg, J. (1958). Myoelastic-aerodynamic theory of voice production. *J. Speech Hear. Res.* **1**, 227-243.
Vergne, A. L., Pritz, M. B. and Mathevon, N. (2009). Acoustic communication in crocodilians: from behaviour to brain. *Biol. Rev.* **84**, 391-411.
Vliet, K. A. (1989). Social displays of the American alligator (*Alligator mississippiensis*). *Am. Zool.* **29**, 1019-1031.
Vogel, P. (1976). Der Stimmapparat der Reptilien, mit besonderer Berueckichtigung von Lacerta galloti. *Verhandlungen der Naturforsch. Gesellschaft Basel* **84**, 135-153.
Wade, J. and Arnold, A. P. (2004). Sexual differentiation of the zebra finch song system. *Ann. NY Acad. Sci.* **1016**, 540-559.
Wang, X. Y., Wang, D., Wu, X. B., Wang, R. P., and Wang, C. I. (2007). Acoustic signals of Chinese alligators (*Alligator sinensis*): social communication. *J. Acoustic. Soc. Am.* **121**, 2984-2989.
West, R. and Larson, C. R. (1993). Laryngeal and respiratory activity during vocalization in macaque monkeys. *J. Voice* **7**, 54-68.
Young, B. A. (2003). Snake bioacoustics: toward a richer understanding of the behavioral ecology of snakes. *Quarterly Rev. Biol.* **78**, 303-326.
Zweers, G. A., van Pelt, H. C. and Beckers A. (1981). Morphology and mechanics of the larynx of the pigeon (*Columba livia* L.): a drill-chuck system. *Zoomorphology* **99**, 37-69.